MODEL VALIDATION OF A TILTWING UAV IN TRANSITION PHASE APPLYING WINDTUNNEL INVESTIGATIONS

J. Holsten*, T. Ostermann*, Y. Dobrev*, D. Moormann*
***Institute of Flight System Dynamics, RWTH Aachen University, Germany**
holsten@fsd.rwth-aachen.de

Keywords: *Tiltwing, Wind tunnel test, Transition phase, UAV*

Abstract

Within the AVIGLE project, funded by the European Union and the German state of North Rhine-Westphalia, the Institute of Flight System Dynamics develops an unmanned aerial vehicle (UAV) in tiltwing configuration. In the transition phase of a tiltwing aircraft the aerodynamic forces and moments, the forces due to the propulsion system and the propeller slipstream induced forces and moments have to be considered and balanced for each stationary flight condition. In this contribution the approach used to model the forces and moments of the transition phase is detailed and the results from the wind tunnel campaign for the AVIGLE tiltwing aircraft are presented and used to validate the design focusing on the transition phase.

Nomenclature and Abbreviations

A_W	Wing area
A_{Prop}	Propeller area
C_L	Lift coefficient
$C_{L,0}$	Lift coefficient without propulsion
$\Delta C_{L,T}$	Additional lift coefficient due to propulsion
D	Overall drag
L	Lift of the complete aircraft
M	Sum of pitching moments
T	Thrust
V_∞	Freestream velocity
V_W	Velocity at the wing
W	Weight
X	Forces in x_f-direction
Z	Forces in z_f-direction
q	Dynamic pressure
x	x-axis specified by index
y	y-axis specified by index
z	z-axis specified by index
α	Angle of attack
ζ	Rudder deflection
η	Elevator deflection
κ	Slipstream flap deflection
ξ	Aileron deflection
ρ	Density
σ	Incidence angle of the wing

Indexes

a	Aerodynamic coordinate system
f	Aircraft fixed coordinate system
i	Induced
W	Wing
T	Thrust, Tailplane
F	Fuselage

1 Introduction

Within the AVIGLE research project funded by the European Union and the German federal state of North-Rhine Westphalia a tiltwing aircraft is being developed. The interaction of thrust and aerodynamic forces and moments during the transition phase of a tiltwing aircraft poses a challenge for modeling and developing control strategies. In this contribution wind tunnel tests to obtain coefficients and derivatives characterizing

the transition phase are described and analyzed.

1.1 AVIGLE Project

Within AVIGLE, which started in 2010 and is funded for three years, 10 project partners from universities and industry work together to develop an avionic digital service platform for different missions. Two main scenarios are considered, one is to gain input data in form of highly resolved pictures for visual applications. The other is providing additional mobile radio communication capabilities. Further information on the mission scenarios, and an overview on the complete system is given in [1].

The Institute of Flight System Dynamics is mainly responsible for the development of the flight platform. The mission requirements on the aerial vehicle demand agility and precise maneuverability, flight velocities from hovering to fast forward flight, high efficiency and endurance, which led to the selection of a tiltwing configuration to best fulfill the needs of the AVIGLE project. Further information on the requirements and the complete design process is given in [2, 3].

1.2 Aircraft Specification

In accordance with the mission requirements a tiltwing aircraft was specified as aerial platform of the AVIGLE project. In contrast to conventional aircrafts a tiltwing can rotate its wings around the aircrafts lateral axis. This also leads to a rotation of the propulsion system, which is fixed on the wing. Depending on the incidence angle of the wing σ the aircraft is able to take-off and land vertically, to hover and to fly efficiently using aerodynamic lift at higher forward velocities.

Key platform parameters of the tiltwing designed within AVIGLE are a maximum take-off weight of 10 kg, an endurance of 60 min and a maximum wing span as well as lateral dimension of 2 m. The basic platform parameters are summarized in Table 1.

A first prototype of the tiltwing was build in June 2011. Due to the limited maximum lateral dimension the propulsion system is located at the middle of the wing, leading to a complete overlap between propeller and wing. Due to this overlap between propeller and wing, the propeller slipstream influences the flow field at the wing and thus the resulting aerodynamic forces and moments.

Table 1 Basic flight platform parameters

Parameter	Values
Configuration	VTOL
Maximum velocity	40 m/s
Design speed	15 m/s
Maximum take-off weight	10 kg
Wing span	2 m
Propeller diameter	0.7 m

2 Transition phase of a tiltwing

The transition phase of a tiltwing includes all flight states between purely aerodynamic horizontal forward flight and hovering. During the transition phase the wing is rotated from horizontal position to vertical position or backwards. Historically, the controllability through a pilot of the aircraft during transition was of major concern [4]. With the development of more sophisticated control algorithms this challenge is met and current development is driven towards time-optimal transitions or optimal transitions with respect to energy [5, 6]. These transitions minimize the time spent in hovering and the time spent at small forward velocities. Furthermore most transition concepts consider the transition as a continuous process. In contrast to this classic tiltwing approach the aim of the AVIGLE aircraft design is to enable a steady trimmed flight at all forward velocities between hovering and stall speed.

2.1 Flight mechanics during transition

The main challenge of flying a steady transition is in the control of the longitudinal forces and moments. To ensure a stationary trimmed flight condition for all forward velocities within the transition phase the resulting forces X and Z in the longitudinal body axes and the sum of pitching

moments M have to be to zero

$$X, Z, M = 0. \tag{1}$$

Main forces acting along the $x-$ and $z-$axis are the corresponding components of the trust T, weight W, lift L, consisting of the lift of the wing L_W, tailplane L_T and fuselage L_F and drag D. An overview of the acting forces and geometric data is given in Figure 1. During transition from hovering, where the wing is tilted to $\sigma = 90°$, to aerodynamic horizontal flight with incidence angles close to $\sigma = 0°$ the thrust is continuously reduced, while the lift grows with increasing forward velocity. Since the thrust vector does not act in the center of gravity an additional pitching moment occurs. At small forward velocities the elevator does not supply enough control to balance the pitching moment. Due to the large thrust the propellers produce sufficient slipstream to use the ailerons for yaw control and depending on the geometric design for pitch control in these flight states. An impeller is included for additional pitch control at low forward velocities. At higher forward velocities the elevator provides sufficient pitch control.

During the design phase the balance of forces and moments was modeled for the transition phase as described in [3]. Aerodynamic coefficients obtained by computation and a momentum theory estimation of the propeller slipstream were used. Through variation of the incidence angle σ, the thrust setting T and flap deflections trimmed conditions for different horizontal and vertical velocities were calculated. These combinations of σ, T and V_∞ were also used as basis for the measurement matrix of the wind tunnel tests as detailed in Section 3. Relevant trimmed conditions are depicted in Figure 2.

2.2 Aerodynamics during transition

Due to the large propeller and low forward velocities during transition the propeller induced slipstream influences the flow field at the wing significantly. This leads to a lower angle of attack at the wing and an accelerated flow field and thus pushes the flow separation to higher angles

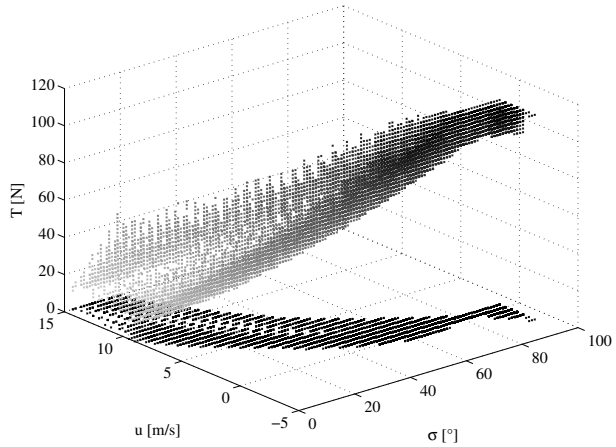

Fig. 2 Trimmed conditions for the transition phase [3].

of attack. In Figure 1 the freestream velocity V_∞ and the resulting velocity at the wing V_W are indicated. Furthermore, during transition phase to vertical flight the thrust is increased, leading to a higher slipstream velocity while the forward velocity is reduced. As soon as freestream velocity and slipstream velocity reach about the same size the interference and influence on the aerodynamic forces is largest.

For conventional aircraft requiring less thrust than a tiltwing configuration during transition phase and where the overlap between propeller and wing is smaller the aerodynamic forces and moments are often described using coefficients and derivatives, for example the lift coefficient C_L defined as

$$C_L = \frac{L}{q \cdot A_W}, \tag{2}$$

with the dynamic pressure $q = \rho/2\, V_\infty^2$ and the wing area A_W. For conventional aircraft C_L only depends on the angle of attack α, the aircraft design and the flap and control device deflection. C_L can easily be determined through wind tunnel measurements at one unique freestream velocity representing the correct Reynolds number or by means of numerical calculations.

As mentioned above in case of a tiltwing several factors complicate the determination of the aerodynamic forces. The smallest complication is the significant change of the aircraft configuration as a result of tilting the wing. To con-

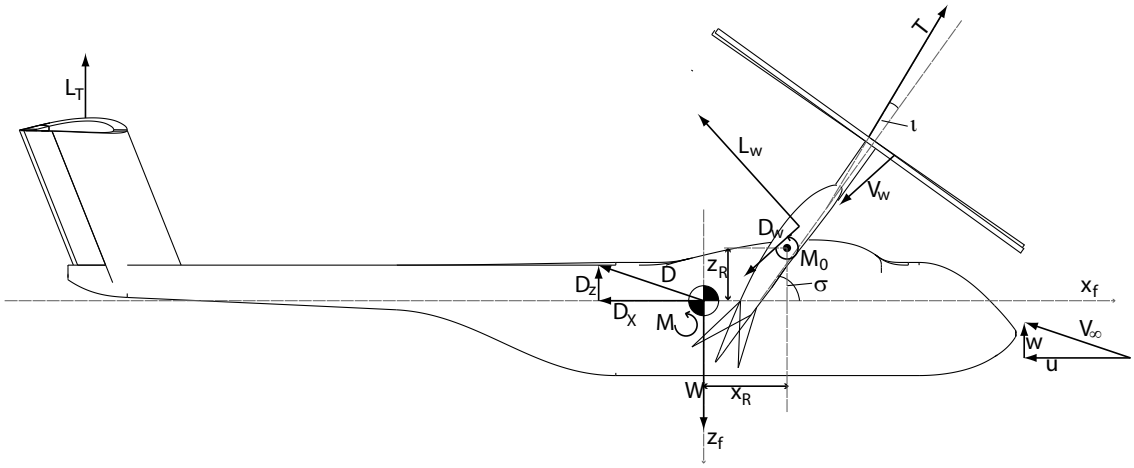

Fig. 1 Forces acting in tilted position [3].

sider this effect in the determination of the coefficients multiple measurements for different incidence angles are to be conducted. Additionally the influence of the propeller slipstream on the flow field around the wing cannot be neglected as usually done. This influence mainly depends on the freestream velocity, the incidence angle of the wing and the thrust and is not fully determined yet. This means all aerodynamic forces and moments e.g.

$$L = f\left(V_\infty, \alpha, \sigma, T\right), \tag{3}$$

depend on the freestream velocity V_∞, α, σ and the thrust T.

3 Wind tunnel measurements

For verification of the design, identification of the aircraft, and to better understand the influence of the propeller slipstream for this specific tiltwing configuration dedicated wind tunnel tests were carried out before flight tests are conducted. Especially building a database for a 6-degrees of freedom (6-dof) simulation, which then is used for control law design, is an important aim of the measurements. Disadvantages of wind tunnel tests compared to free flight tests are the fixation of the aircraft and thus in most cases it is only possible to determine the static coefficients and derivatives. Furthermore depending on the size of the aircraft and the wind tunnel scaling effects have to be considered. Advantages of wind tunnel tests compared to free flight tests are the precisely known freestream and attitude conditions and the possibility to use a smaller model and thus save costs as well as reducing the risk of destroying a first prototype in free flight tests.

For conventional aircrafts the coefficients and derivatives of the aircraft without propulsion system are determined and the through the propulsion system acting forces and moments are added using superposition. The advantage is, that usually one freestream velocity is sufficient to determine the aerodynamic coefficients according to Equation 2.

3.1 Wind tunnel used

The Institute of Flight System Dynamics has a closed circuit wind tunnel with an open measurement area, where models up to a size of 1 m in wingspan can be identified. The freestream velocity can be adjusted from a few $^{\mathrm{m}}/_{\mathrm{s}}$ up to $\approx 70\,^{\mathrm{m}}/_{\mathrm{s}}$. For determination of the aerodynamic coefficients the resulting forces and moments in all three dimensions can be measured using a balance with strain gauges.

Due to the size of the wind tunnel a 1 : 2 scaled model of the AVIGLE tiltwing was used. Different control factors of the sub scale model such as thrust, control devices, incidence an-

gle of the wing, engine pod and elevator were built as adjustable control elements. To ensure Reynolds similarity a scaled model requires a higher freestream velocity. For correct measurement of the slipstream flap coefficients and derivatives as well as the interaction the propeller size was scaled with the model in an 1 : 2 ratio. This also ensures the same overlap between wing and propellers in the scaled model as in the original model.

Scaling the propeller size geometrically and doubling the slipstream velocity to ensure Reynolds' similarity leads to the same amount of thrust for the scaled and original model when applying momentum theory [7], and neglecting the freestream velocity in the calculation. Estimating the propeller slipstream at different angles of attack and different freestream velocities is only iteratively possible. Therefore the measured interaction as well as the calculated slipstream have to be treated carefully.

Even regarding these simplifications for a complete dataset the thrust and the freestream velocity would have to be varied for all incidence angles leading to a set of measurement points over $[\alpha, \sigma, V, T, \kappa]$, for only the longitudinal motion where κ stands for all flap and control device deflections respectively. To reduce the measurement time in the wind tunnel and still gain a significant dataset the model as described in the following section was applied.

3.2 Measurement setup and data evaluation

For simulation purposes, control strategies and validation a separation into purely aerodynamic forces and moments, forces and moments due to thrust settings and additional forces and moments due to the propeller slipstream is essential. Especially the additional forces cannot be measured directly with a scaled model in wind tunnel tests due to the above mentioned factors. Furthermore, measuring the complete dataset by varying all parameters would take too much time in the wind tunnel.

To gain a good estimate of the different forces and moments three sets of measurements were conducted. First the purely aerodynamic model without propulsion system was measured at one freestream velocity for different $[\alpha, \sigma, \kappa]$. Then the scaled propulsion system was measured for incidence angles ranging from 0° to 90° with a step size of 5° to cover all incidence angles of the wing. The step size was chosen since the scaled aircraft model only allows changes in the incidence angle of 5°. These measurements were conducted at freestream velocities depending on the incidence angle as given in Table 2, which were determined according to prior wind tunnel measurements and the calculations visualized in Figure 2, taking into consideration existing resonance vibrations and the scaling due to Reynolds similarity.

Table 2 Chosen correlation of freestream velocity and incidence angle.

$\sigma\,[^\circ]$	$[0;20]$	$[25]$	$[30;45]$	$[50;55]$	$[60;90]$
$V\,[\mathrm{m/s}]$	30	25	20	15	10

Last the scaled model including propulsion system was measured over the same range of σ and V_∞ while varying the following parameters $[\alpha, \kappa, T]$. The thrust was set within $[0\,\mathrm{N}; 40\,\mathrm{N}]$. In the thrust the drag of the propeller is included. The thrust setting to achieve a thrust of 0 N increases with the freestream velocity since the wind mill stadium of the propeller has to be overcome and reflects no real flight state but was included as a lower bound.

For simulation and also for model validation two datasets were generated representing the above mentioned purely aerodynamic forces and moments and the forces and moments additionally induced by the propeller slipstream. The trust remains in all cases as an independent control parameter. The purely aerodynamic coefficients are calculated from the "clean" measurements according to the standard definition

$$C_{L0} = \frac{X_a}{\rho/2\, V_\infty^2\, A_W}, \tag{4}$$

in the following always indicated through the index $_0$.

From the combined measurements a first coefficient C_L is calculated according to Equation 4. From this coefficient then the clean coefficient C_{L0} and the corresponding thrust components are subtracted, as given in Equation 5. Afterwards the coefficients are related to the overall dynamic pressure q_{total} resulting in by thrust induced coefficients, e.g.

$$\Delta C_{L,T} = \left(C_L - C_{L0} - \frac{T \cdot \sin(\sigma + \iota)}{A_W \cdot q_\infty} \right) \cdot \frac{q_\infty}{q_{\text{total}}}. \tag{5}$$

These induced additional coefficients are related to the overall dynamic pressure consisting of the sum of the freestream velocity V_∞ and the propeller induced slipstream V_i

$$q_{\text{total}} = \frac{\rho}{2} \left(V_\infty^2 + V_i^2 \right), \tag{6}$$

with V_i resulting from the momentum theory

$$V_i = \sqrt{\frac{2\,T}{A_{\text{Prop}}\,\rho}}, \tag{7}$$

where A_{Prop} is the propeller area. The additional coefficients are related to the overall velocity at the wing and not as is convention to the freestream velocity to account for small freestream velocities up to a freestream velocity of $V_\infty = 0\,\text{m/s}$, where additional forces and moments only occur due to the propeller slipstream.

Using this model the following simplification and assumptions were made:

- Neglect of V_∞ in the calculation of V_i
- Simplifications made in the momentum theory [7]
- Scalar instead of vectorial sum of velocities is made
- Incorrect reference to α since the angle of attack at the wing α_W is also influenced by V_i and thus $\alpha_W \neq \alpha$.

With these simplifications in mind it is now possible to generate two datasets of coefficients based on the finite number of wind tunnel tests. The dataset of purely aerodynamic forces and moments depends on $[\alpha, \kappa, \sigma]$ and has to be scaled by q_∞ and the dataset of additional forces and moments depends on $[\alpha, \kappa, \sigma, T]$ and is scaled by an estimate of the total dynamic pressure at the wing q_{total}. The thrust T was selected as additional parameter, since it could be set with a good repeatability during the measurements. Hence an easy correlation to the thrust measurements is possible. Instead of the thrust it would also be possible to use the total velocity or a relation of freestream velocity to propeller induced slipstream.

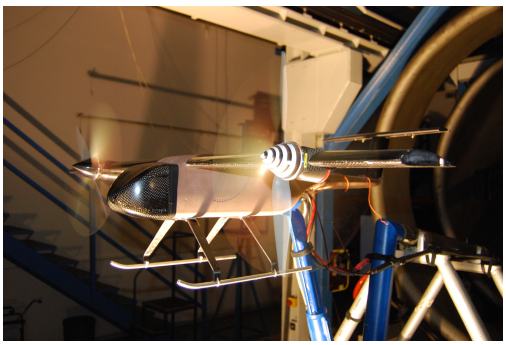

Fig. 3 Setup of the wind tunnel measurements.

An overview on the parameters set during the wind tunnel tests is given in Table 3. The setup of the sub scale model in the wind tunnel is given in Figure 3.

Table 3 Parameters set during the wind tunnel tests.

	Range	Step Size
V [m/s]	[10;30]	5
T [N]	[10;40]	10
σ [°]	[0;90]	5
α [°]	[−5;20]	5
κ, ξ [°]	[−16;16]	4
η, ζ [°]	[−20;20]	4

4 Results

For validation of the tilwing model dataset as used in the 6-dof simulation all measured data from the wind tunnel campaign was analyzed analytically. Relevant for the transition is especially

the longitudinal movement. Therefore only the results for lift, drag and pitch moment coefficients will be discussed as well as the resulting forces in $x-$ and $z-$ direction.

4.1 Lift

Figure 4 illustrates the influence of the incidence angle σ on the lift coefficient $C_{L,0}$ for different angles of attack α. In this case the propulsion system was not included in the measurements. It

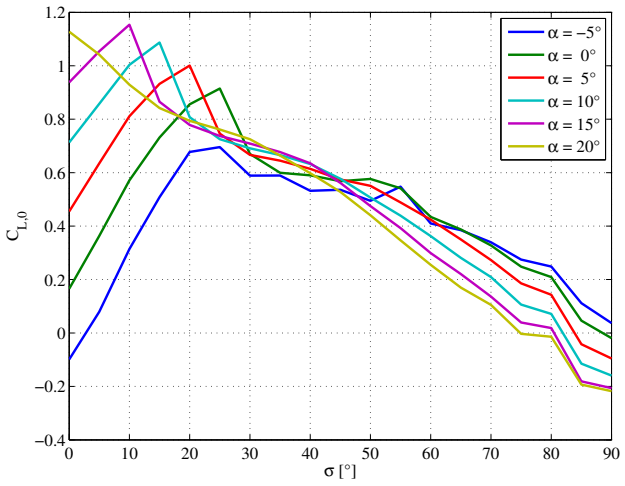

Fig. 4 $C_{L,0}$ over σ for varying α.

can be seen, that at first an increase of σ leads to an increase in lift, similar, though a little bit less than an increase in α. The difference in value can be explained by the tailplane which contributes to the overall lift, but is hardly influenced by σ. After flow separation the lift coefficient decreases continuously, as would be expected.

Considering the lift coefficient $\Delta C_{L,T}$, which is additionally induced by the thrust, the maximum value is shifted to higher σ as illustrated in Figure 5. The slipstream of the propellers, which is proportional to the thrust given in Figure 5, shifts the separation of the flow at the wing to higher σ. This allows the usage of less thrust during the transition.

A thorough model validation of the transition phase can only be done in the simulation. To gain a first insight into the overall forces in $z-$direction the dataset was used to calculate Z for varying thrust and freestream velocities. The

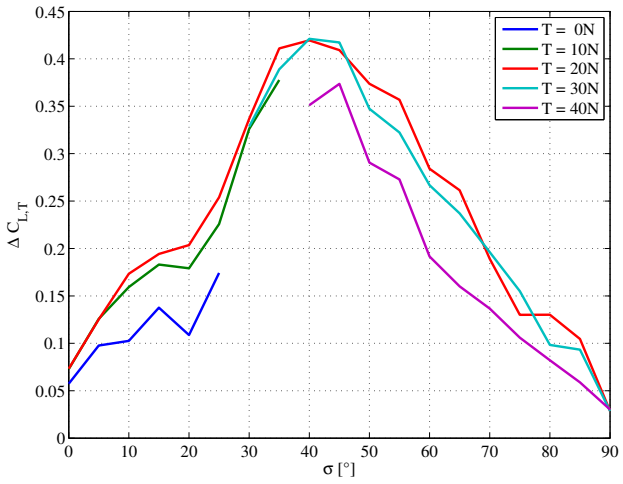

Fig. 5 $\Delta C_{L,T}$ over σ for varying T.

results are illustrated in Figure 6. It has to be noted that in the depicted case $\alpha = 0^\circ$ and no control device deflection was regarded.

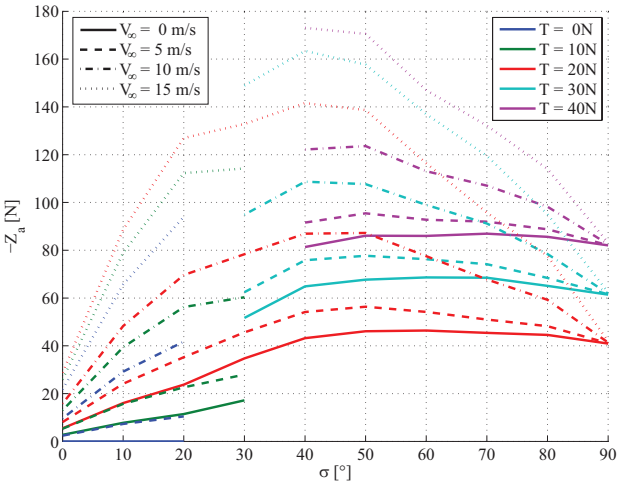

Fig. 6 Overall vertical force over σ, T and V_∞.

Depending on the weight of the aircraft $Z \approx 100\,\mathrm{N}$ for a trimmed flight without loosing height. Further variation of Z can be achieved through a change of α or control device deflection.

4.2 Drag

The influence of σ on $C_{D,0}$ and $\Delta C_{D,T}$ is illustrated in Figure 7 and 8. An increase of σ consequently leads to an increase of $C_{D,0}$. For $\Delta C_{D,T}$ it can be seen that for smaller σ the additional drag coefficient is partially reduced. For higher

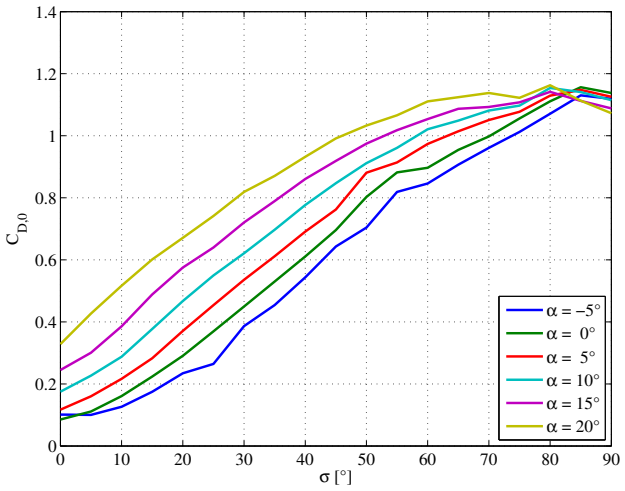

Fig. 7 Influence of σ on $C_{D,0}$ for different α.

σ $\Delta C_{D,T}$ increases. Through the induced flow around the wing additional lift L_W, as indicated in Figure 1, is created. When transforming this lift with σ into aircraft and aerodynamic coordinates it acts in negative x_a-direction and thus increases the drag. Another aspect influencing the additional drag coefficient is the subtraction of the thrust. The thrust was measured without the influence of the wing. The actual thrust during the measurements can be assumed to be a little bit smaller and thus resulting in larger additional drag coefficients. Still this effect can be regarded as small compared to the induced L_W.

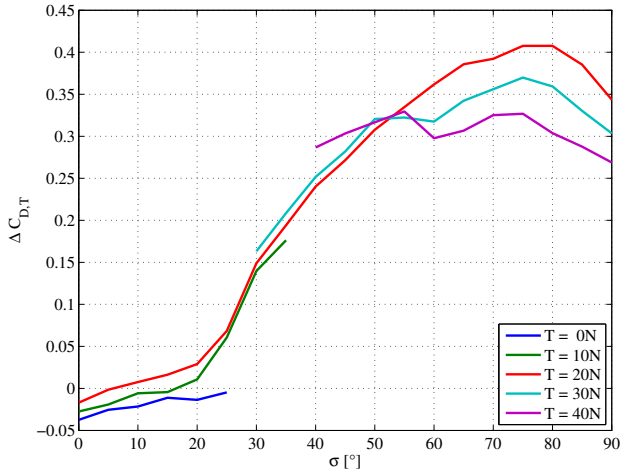

Fig. 8 Influence of σ on ΔC_D for different T.

Figure 9 illustrates the overall drag for the same settings as for the lift illustrated in Figure 6.

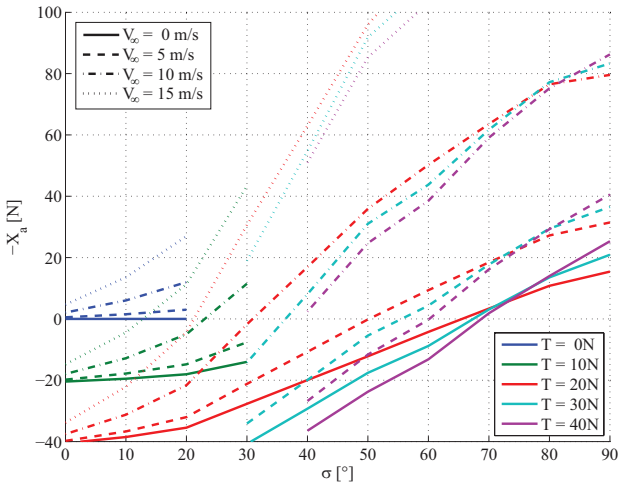

Fig. 9 Overall horizontal force for different σ, T and V_∞.

It can be seen that for all velocities depicted a trimmed condition in the x_a-axis can be achieved.

Overall it can be noted that the large propeller and special flow conditions during the transition have a positive effect on the overall lift, but a negative on the overall drag. To find trimmed conditions for X, Z and M further investigations using a 6-dof simulation and additional wind tunnel tests are necessary.

4.3 Pitching moment

Balancing the overall forces in $x-$ and $z-$direction is possible by adjusting the incidence angle σ and the thrust T to the desired forward velocity V_∞. During design it was considered to balance the pitching moment only through slipstream flaps and at higher velocities through the elevator. The pitching moment is largely influenced by the lift and drag and the geometric design of the overall plane. Additionally a change in incidence angle leads to a shift in geometric distances of the resulting forces to the center of gravity. The additional pitching moment for different incidence angles is given in Figure 10.

The tendencies of the additional drag and lift coefficient can be seen at $\sigma \approx 25^\circ$ and $\sigma \approx 50^\circ$. Due to the relatively close location of the slipstream flaps to the center of gravity their effect

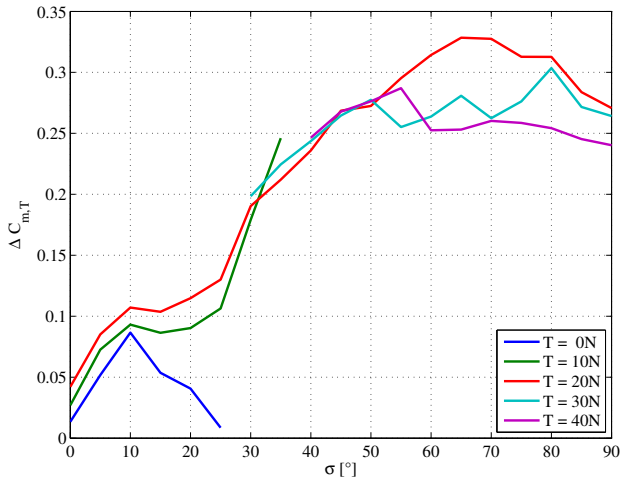

Fig. 10 $\Delta C_{m,T}$ over σ and T.

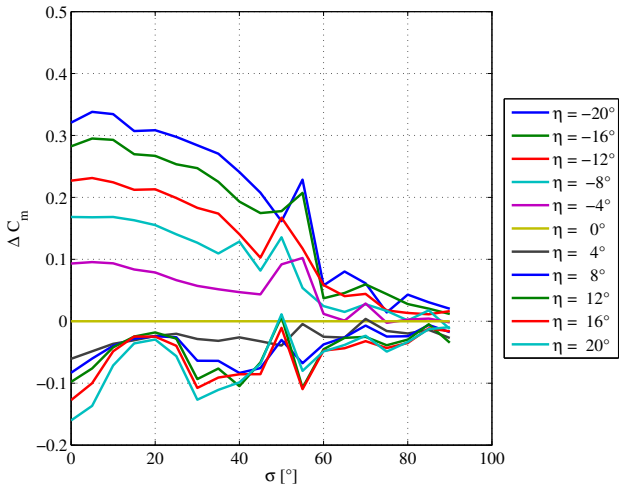

Fig. 12 Influence of η on ΔC_m for different σ.

on the pitching moment is very small. The influence of symmetrical deflection is visualized in Figure 11. It has to be noted that $\Delta C_{m,T}$ is not 0 for $\kappa = 0\,^\circ$ since the propeller slipstream induces a pitching moment of the wing which is included in this coefficient and equals $\Delta C_{m,T}$ depicted in Figure 10.

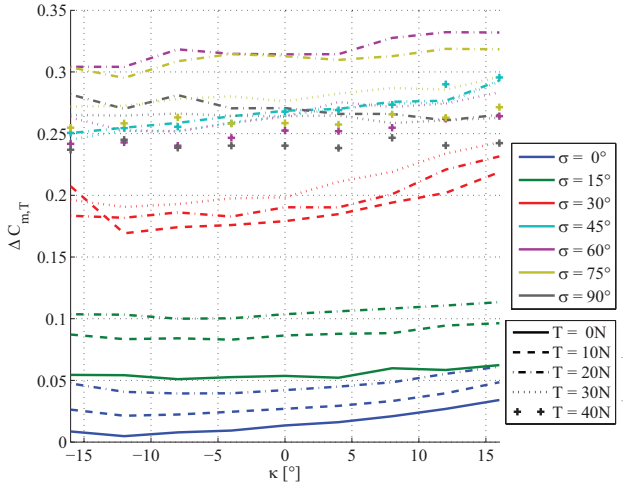

Fig. 11 Influence of κ on $\Delta C_{m,T}$ for different σ and T.

The influence of the elevator deflection η on the pitching moment is visualized in Figure 12. $\Delta C_{m,\eta}$ decreases with increasing σ, since part of the freestream is blocked by the tilted wing. Furthermore for higher σ the freestream velocity V_∞ decreases and since the moment through η is only marginally influenced through the slipstream its effectiveness decreases with higher σ. Another effect to be considered is the influence of the separation bubble of the wing reaching the elevator at $\sigma \approx 20\,^\circ$.

In the first prototype especially for transition and vertical flight an additional impeller is included to balance the small effectiveness of the slipstream flaps.

5 Conclusion

In this paper the challenges in creating a validated model for a tiltwing in transition phase between vertical and horizontal flight using wind tunnel tests have been described. After an overview on the used tiltwing design and flight dynamical and aerodynamical aspects within transition phase a model identification and measurement approach to determine coefficients representing aerodynamic as well as propeller induced forces and moments was detailed. The coefficients were then used to validate the tiltwing design itself and to serve as a basis for control laws design.

According to the presented results trimming the pitching moment applying solely slipstream flaps during the transition phase remains a challenge. However it has to be noted that the used method for coefficient calculation as well as the wind tunnel measurements are afflicted with uncertainties. Due to the scaling of the wind tunnel model cut backs on the propulsion system had to

be made.

In future additional wind tunnel and free flight tests are planned to specify the influence of flaps and control devices more precisely. Wind tunnel tests investigating the influence of different velocities on the induced forces are also planned for the future. In this contribution the influence of the freestream velocity was only modeled theoretically. Furthermore, a 6-dof simulation will be used to investigate possible transition methods and to further validate the tiltwing design and dataset calculation. Free flight tests of the transition phase are planned for the near future.

Acknowledgment

Our work has been conducted within the AVIGLE project, which is part of the Hightech.NRW research program funded by the German Ministry for Innovation, Science and Research in North Rhine-Westphalia and the EU. AVIGLE is conducted in cooperation with several industrial and academic partners. We thank all project partners for their work and contributions to the AVIGLE project.

Ministry for Innovation, Science and Research of North Rhine-Westfalia

EUROPEAN UNION

European Regional Development Fund

Copyright Statement

References

[1] S. Rohde, N. Goddemeier, C. Wietfeld, F. Steinicke, K. Hinrichs, T. Ostermann, J. Holsten, D. Moormann, AVIGLE: A System of Systems Avionic Digital Service Platform Based on Micro Unmanned Aerial Vehicles, in *IEEE International Conference on Systems, Man, and Cybernetics (SMC)*, Instanbul, Turkey, October 2010

[2] T. Ostermann, J. Holsten, D. Moormann, Entwicklung eines autonom operierenden Tiltwing-UAV fuer den Einsatz in selbstorganisierenden Drohnenschwaermen = Development of an Autonomous Tiltwing UAV for the Operation in Self-organized Drone Swarms, in *Deutscher Luft- und Raumfahrtkongress 2010 : Hamburg, 31.8. - 02.09.2010; Tagungsband - Ausgewaehlte Manuskripte* (DGLR, Bonn, 2010)

[3] J. Holsten, T. Ostermann, D. Moormann, Design and wind tunnel tests of a tiltwing UAV, in *CEAS Aeronautical Journal*, Springer Wien, Vol. 2, pp. 69-79,2011

[4] L. P. Thomas III, *A Flight Study of the Conversion Maneuver of a Tiltwing VTOL Aircraft*. NASA-TN-D-153, 1959.

[5] H. Friedel, K. Stopfkuchen *Ein Verfahren zur Berechnung zeitoptimaler Übergangsflüge von VTOL-Flugzeugen = A Method of Calculation of Time Optimal VTOL Transition Flights*. Jahrbuch der WGLR, 1963.

[6] G. Bruening, *Zur zeitoptimalen Transition von VTOL-Flugzeugen = About Time Optimal VTOL Transition Flights*. Z. Flugwiss. 14, 1966.

[7] W. Johnson, *Helicopter Theory* (Princeton University Press, 1980)